

## Development and Validation of the New Continuous Energy Capability in the Criticality Safety Code KENO

Sedat Goluoglu<sup>a,\*</sup>, Michael E. Dunn<sup>a</sup>, Lester M. Petrie<sup>a</sup>, and Tyler S. Sumner<sup>b</sup>

<sup>a</sup> Oak Ridge National Laboratory, Oak Ridge, Tennessee, USA

<sup>b</sup> Georgia Institute of Technology, Atlanta, Georgia, USA

---

### Abstract

The continuous energy cross sections that are used in KENO V.a and KENO-VI are generated using the latest AMPX cross-section processing system. ENDF/B-VI Release 8 and ENDF/B-VII Release 0 data have recently been processed through AMPX to generate continuous energy cross-section data. Continuous energy versions of KENO and these newly generated data have been tested using various problem sets, including SCALE sample problems and critical benchmark cases. Analysis of the results from continuous energy KENO V.a and continuous energy KENO-VI using the latest AMPX-generated ENDF/B-VII Release 0 cross sections are presented for benchmark problems that represent a wide range of critical fissile systems.

---

### 1. Introduction

Oak Ridge National Laboratory (ORNL) has incorporated continuous energy capability in the KENO V.a and KENO VI codes that are maintained as part of the Standardized Computer Analyses for Licensing Evaluation (SCALE) code system (SCALE, 2006). Both codes can perform the neutron transport calculations in either multigroup or continuous energy mode. The energy treatment mode is automatically selected based on the cross-section library name if the problem is initiated by one of the corresponding control modules. For KENO V.a the control module is CSAS5; for KENO-VI the control module is CSAS6. In the remainder of this paper, when the KENO code is referenced, calculation in the continuous energy mode is implied.

As part of this development, ORNL has developed a continuous energy cross-section format and the continuous energy cross-section processing software needed to prepare data libraries for KENO. The processing software has been added to the AMPX (Dunn and Greene, 2002) code system that is used to prepare nuclear data libraries for SCALE. Production continuous energy libraries based on ENDF/B-VI Release 8 and ENDF/B-VII Release 0 evaluations have been prepared using the AMPX code system. Both sets of cross sections have been generated at multiple temperatures: 300, 600, 900, 1200, and 2400 K. In addition, the cross sections for the nuclides with thermal scattering data have been generated at the temperatures that are provided in the corresponding ENDF/B evaluation files. Although temperature interpolation of the cross sections is not yet available in the continuous energy

---

\* Corresponding author, [goluoglus@ornl.gov](mailto:goluoglus@ornl.gov)  
Tel: (865) 574-5255; Fax: (865) 576-3513.

mode of KENO, having multiple temperature cross sections available allows more accurate (albeit possibly approximate) analysis of high-temperature systems. As part of the benchmarking effort, critical benchmark experiments that include a wide variety of fissile systems in various moderator and reflector configurations have been selected.

This paper provides the results of initial validation efforts for KENO and the corresponding continuous energy cross-section data that are based on the ENDF/B-VII Release 0 evaluations for more than 500 benchmark problems. These benchmark problems provide a comprehensive validation suite. Goluoglu et al. (2007) have previously reported the performance of the code and continuous energy cross sections based on ENDF/B-VI Release 8 for a limited number of benchmarks.

## 2. Benchmark Problems

Benchmark problems that have been used in this study have been selected to provide a validation suite from a wide range of fissile systems. The benchmark problems have been divided into six groups: High enriched uranium systems (HEU), intermediate enriched uranium systems (IEU), low enriched uranium systems (LEU), mixed oxide systems (MOX), plutonium systems (Pu), and  $^{233}\text{U}$  systems (U-233). The benchmark problems are from the *International Handbook of Evaluated Criticality Safety Benchmark Experiments (IHECSBE)* (2007). The case filenames in the following sections are based on the *IHECSBE* naming conventions with minor changes. Since the benchmark problems are from the *IHECSBE*, detailed model descriptions have not been provided in this paper. Rather, the reader is referred to the documentation provided with the *IHECSBE*.

## 3. Validation and Results

A total of 515 benchmark problems have been modeled and analyzed in six groups. The following sections provide detailed analysis results for these benchmark groups. All KENO calculations used continuous energy cross sections based on ENDF/B-VII Release 0 evaluations and have been run with a sufficient total number of histories to

achieve a standard deviation of  $k_{\text{eff}}$  of 0.0005 or less. In the following sections, the percent differences have been adjusted to account for the uncertainty in the calculated  $k_{\text{eff}}$  values and the uncertainty in the benchmark  $k_{\text{eff}}$  values.

### 3.1. HEU

This group consists of 184 HEU systems. The calculated  $k_{\text{eff}}$  values and percent differences are shown in Fig. 1 to identify cases that show poor agreement. Table 1 lists the benchmark filenames,  $k_{\text{eff}}$  values, and KENO calculated  $k_{\text{eff}}$  values.

The vast majority of the benchmarks in this group are calculated very accurately.

The hci005 series benchmarks show poor agreement. Three of the cases that show poor agreement are noted below. These benchmarks also have unusually high benchmark  $k_{\text{eff}}$  values (greater than 1.0). Clearly, the values were extrapolated; a benchmark  $k_{\text{eff}}$  value of even 1.03 (for hci005.1) implies a super prompt critical configuration that would not be possible for a critical benchmark experiment in a laboratory. A review of the corresponding evaluation document from the *IHECSBE* has been performed to determine the cause of these large discrepancies. The evaluators of the hci005 series experiments report similar large discrepancies with various codes and cross-section data sets and believe that the problem is with the cross sections for the structural materials such as iron, chromium, nickel, and zirconium.

The next set of benchmarks that show large discrepancies is from the hmf007 series (cases 32, 33, and 34). These three cases are the only cases from the hmf007 series that contain a Teflon ( $\text{CF}_2$ ) moderator. Sample calculations that have been provided by the evaluators also show large discrepancies between the calculated and measured benchmark  $k_{\text{eff}}$  values for these cases. Therefore, it is likely that fluorine cross sections are the reason for overestimating their  $k_{\text{eff}}$  values.

The benchmark hmf060 is also poorly calculated. Evaluators for this benchmark report similarly high calculated values for this configuration, which is a cylindrical assembly of U metal (93%  $^{235}\text{U}$ ) and tungsten with aluminum reflectors (also identified as ZPR-9, assembly 4).

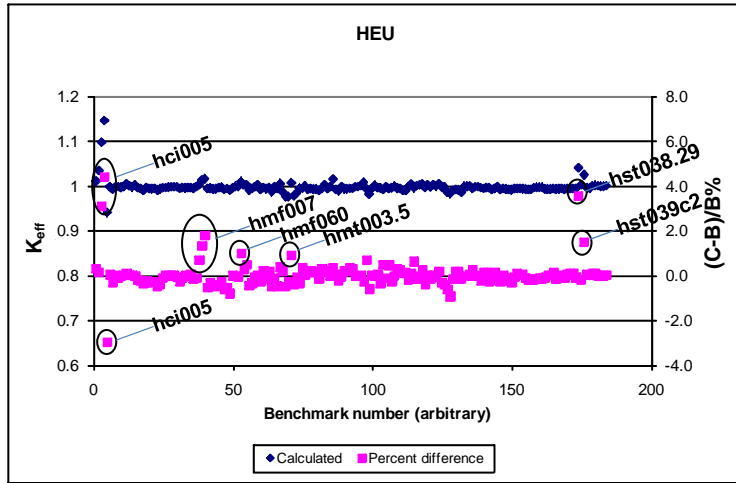


Fig. 1. Calculated  $k_{\text{eff}}$  values and percent differences for HEU benchmarks.

Table 1  
Calculated  $k_{\text{eff}}$  values and percent differences for HEU benchmarks

| Benchmark |             |                  |             | KENO-CE          | Benchmark |              |                  |             | KENO-CE          |
|-----------|-------------|------------------|-------------|------------------|-----------|--------------|------------------|-------------|------------------|
| No.       | Name        | $k_{\text{eff}}$ | Uncertainty | $k_{\text{eff}}$ | No.       | Name         | $k_{\text{eff}}$ | Uncertainty | $k_{\text{eff}}$ |
| 1         | hci004      | 1.0000           | 0.0040      | 1.0110           | 36        | hmf007-30    | 0.9981           | 0.0002      | 0.9955           |
| 2         | hci005.1    | 1.0320           | 0.0040      | 1.0343           | 37        | hmf007-31    | 1.0013           | 0.0002      | 0.9989           |
| 3         | hci005.2    | 1.0500           | 0.0080      | 1.0984           | 38        | hmf007-32    | 0.9959           | 0.0001      | 1.0038           |
| 4         | hci005.4    | 1.0640           | 0.0180      | 1.1466           | 39        | hmf007-33    | 0.9995           | 0.0001      | 1.0135           |
| 5         | hci005.5    | 0.9970           | 0.0130      | 0.9413           | 40        | hmf007-34    | 0.9977           | 0.0001      | 1.0165           |
| 6         | hmf001.bare | 1.0000           | 0.0010      | 0.9993           | 41        | hmf007-35    | 1.0011           | 0.0001      | 0.9946           |
| 7         | hmf007-01   | 0.9971           | 0.0001      | 0.9929           | 42        | hmf007-36    | 0.9999           | 0.0001      | 0.9956           |
| 8         | hmf007-02   | 0.9986           | 0.0001      | 0.9983           | 43        | hmf007-37    | 0.9988           | 0.0001      | 0.9935           |
| 9         | hmf007-03   | 1.0012           | 0.0001      | 0.9988           | 44        | hmf007-38    | 1.0000           | 0.0001      | 0.9940           |
| 10        | hmf007-04   | 0.9970           | 0.0001      | 0.9976           | 45        | hmf007-39    | 1.0018           | 0.0001      | 0.9967           |
| 11        | hmf007-05   | 1.0000           | 0.0001      | 0.9991           | 46        | hmf007-40    | 1.0013           | 0.0001      | 0.9975           |
| 12        | hmf007-06   | 1.0028           | 0.0001      | 1.0047           | 47        | hmf007-41    | 0.9994           | 0.0001      | 0.9923           |
| 13        | hmf007-07   | 0.9996           | 0.0001      | 1.0008           | 48        | hmf007-42    | 1.0016           | 0.0001      | 0.9949           |
| 14        | hmf007-08   | 0.9992           | 0.0001      | 0.9981           | 49        | hmf007-43    | 0.9998           | 0.0001      | 0.9906           |
| 15        | hmf007-09   | 1.0017           | 0.0008      | 1.0022           | 50        | hmf022       | 1.0000           | 0.0019      | 0.9959           |
| 16        | hmf007-10   | 1.0000           | 0.0001      | 0.9969           | 51        | hmf027       | 1.0000           | 0.0025      | 0.9997           |
| 17        | hmf007-11   | 0.9982           | 0.0001      | 0.9949           | 52        | hmf028       | 1.0000           | 0.0030      | 0.9982           |
| 18        | hmf007-12   | 0.9951           | 0.0001      | 0.9905           | 53        | hmf060       | 0.9955           | 0.0024      | 1.0102           |
| 19        | hmf007-13   | 1.0009           | 0.0001      | 0.9974           | 54        | hmf067.1     | 0.9959           | 0.0024      | 1.0032           |
| 20        | hmf007-14   | 0.9983           | 0.0001      | 0.9941           | 55        | hmf067.2     | 0.9938           | 0.0024      | 1.0034           |
| 21        | hmf007-15   | 0.9978           | 0.0001      | 0.9938           | 56        | hmi006.1     | 0.9977           | 0.0008      | 0.9912           |
| 22        | hmf007-16   | 0.9988           | 0.0001      | 0.9949           | 57        | hmi006.2     | 1.0001           | 0.0008      | 0.9947           |
| 23        | hmf007-17   | 0.9972           | 0.0001      | 0.9913           | 58        | hmi006.3     | 1.0015           | 0.0009      | 0.9987           |
| 24        | hmf007-18   | 0.9991           | 0.0001      | 0.9939           | 59        | hmi006.4     | 1.0016           | 0.0008      | 1.0030           |
| 25        | hmf007-19   | 0.9983           | 0.0001      | 0.9962           | 60        | hmm005.1     | 1.0007           | 0.0027      | 0.9922           |
| 26        | hmf007-20   | 0.9981           | 0.0001      | 0.9971           | 61        | hmm005.2     | 1.0003           | 0.0028      | 0.9967           |
| 27        | hmf007-21   | 0.9987           | 0.0001      | 0.9978           | 62        | hmm005.3     | 1.0012           | 0.0029      | 0.9938           |
| 28        | hmf007-22   | 0.9994           | 0.0001      | 0.9983           | 63        | hmm005.4     | 1.0016           | 0.0030      | 0.9973           |
| 29        | hmf007-23   | 0.9993           | 0.0001      | 0.9982           | 64        | hmm005.5     | 1.0005           | 0.0040      | 0.9874           |
| 30        | hmf007-24   | 1.0001           | 0.0001      | 0.9982           | 65        | hmt001detail | 1.0010           | 0.0060      | 0.9988           |
| 31        | hmf007-25   | 0.9990           | 0.0001      | 0.9952           | 66        | hmt001simple | 1.0010           | 0.0060      | 0.9952           |
| 32        | hmf007-26   | 0.9997           | 0.0001      | 0.9974           | 67        | hmt003.1     | 1.0000           | 0.0010      | 1.0059           |
| 33        | hmf007-27   | 0.9965           | 0.0002      | 0.9960           | 68        | hmt003.2     | 0.9910           | 0.0030      | 0.9869           |
| 34        | hmf007-28   | 0.9987           | 0.0002      | 0.9974           | 69        | hmt003.3     | 0.9826           | 0.0060      | 0.9768           |
| 35        | hmf007-29   | 0.9978           | 0.0002      | 0.9971           | 70        | hmt003.4     | 0.9876           | 0.0040      | 0.9768           |

Table 1  
Calculated  $k_{\text{eff}}$  values and percent differences for HEU benchmarks (continued)

| Benchmark |               |                  |             | KENO-CE          | Benchmark |           |                  |             | KENO-CE          |
|-----------|---------------|------------------|-------------|------------------|-----------|-----------|------------------|-------------|------------------|
| No.       | Name          | $k_{\text{eff}}$ | Uncertainty | $k_{\text{eff}}$ | No.       | Name      | $k_{\text{eff}}$ | Uncertainty | $k_{\text{eff}}$ |
| 71        | hmt003.5      | 0.9930           | 0.0030      | 1.0078           | 128       | hst004.2  | 1.0000           | 0.0036      | 0.9833           |
| 72        | hmt003.6      | 0.9889           | 0.0030      | 0.9787           | 129       | hst004.3  | 1.0000           | 0.0039      | 0.9905           |
| 73        | hmt003.7      | 0.9919           | 0.0030      | 0.9849           | 130       | hst004.4  | 1.0000           | 0.0046      | 0.9924           |
| 74        | hmt006.01     | 1.0000           | 0.0044      | 0.9954           | 131       | hst004.5  | 1.0000           | 0.0052      | 0.9912           |
| 75        | hmt006.02     | 1.0000           | 0.0040      | 0.9952           | 132       | hst004.6  | 1.0000           | 0.0059      | 0.9867           |
| 76        | hmt006.03     | 1.0000           | 0.0040      | 1.0000           | 133       | hst009.1  | 0.9990           | 0.0043      | 0.9996           |
| 77        | hmt006.04     | 1.0000           | 0.0040      | 0.9935           | 134       | hst009.2  | 1.0000           | 0.0039      | 0.9997           |
| 78        | hmt006.05     | 1.0000           | 0.0040      | 0.9940           | 135       | hst009.3  | 1.0000           | 0.0036      | 1.0005           |
| 79        | hmt006.06     | 1.0000           | 0.0040      | 0.9933           | 136       | hst009.4  | 0.9986           | 0.0035      | 0.9940           |
| 80        | hmt006.07     | 1.0000           | 0.0040      | 0.9935           | 137       | hst010.1  | 1.0000           | 0.0029      | 0.9986           |
| 81        | hmt006.08     | 1.0000           | 0.0040      | 0.9903           | 138       | hst010.2  | 1.0000           | 0.0029      | 0.9990           |
| 82        | hmt006.09     | 1.0000           | 0.0040      | 0.9951           | 139       | hst010.3  | 1.0000           | 0.0029      | 0.9967           |
| 83        | hmt006.10     | 1.0000           | 0.0040      | 1.0024           | 140       | hst010.4  | 0.9992           | 0.0029      | 0.9944           |
| 84        | hmt006.11     | 1.0000           | 0.0040      | 0.9941           | 141       | hst013.1  | 1.0012           | 0.0026      | 0.9973           |
| 85        | hmt006.12     | 1.0000           | 0.0040      | 0.9987           | 142       | hst013.2  | 1.0007           | 0.0036      | 0.9969           |
| 86        | hmt006.13     | 1.0000           | 0.0061      | 1.0157           | 143       | hst013.3  | 1.0009           | 0.0036      | 0.9924           |
| 87        | hmt006.14     | 1.0000           | 0.0040      | 0.9922           | 144       | hst013.4  | 1.0003           | 0.0036      | 0.9942           |
| 88        | hmt006.15     | 1.0000           | 0.0040      | 0.9895           | 145       | hst032.1  | 1.0015           | 0.0026      | 0.9987           |
| 89        | hmt006.16     | 1.0000           | 0.0040      | 0.9984           | 146       | hst038.01 | 1.0000           | 0.0025      | 0.9921           |
| 90        | hmt006.17     | 1.0000           | 0.0040      | 0.9939           | 147       | hst038.02 | 1.0000           | 0.0025      | 0.9950           |
| 91        | hmt006.18     | 1.0000           | 0.0040      | 0.9939           | 148       | hst038.03 | 1.0000           | 0.0025      | 0.9935           |
| 92        | hmt006.19     | 1.0000           | 0.0040      | 0.9952           | 149       | hst038.04 | 1.0000           | 0.0025      | 0.9926           |
| 93        | hmt006.20     | 1.0000           | 0.0040      | 0.9950           | 150       | hst038.05 | 1.0000           | 0.0025      | 0.9918           |
| 94        | hmt006.21     | 1.0000           | 0.0040      | 0.9986           | 151       | hst038.06 | 1.0000           | 0.0025      | 0.9941           |
| 95        | hmt006.22     | 1.0000           | 0.0040      | 0.9987           | 152       | hst038.07 | 1.0000           | 0.0032      | 0.9946           |
| 96        | hmt006.23     | 1.0000           | 0.0040      | 1.0008           | 153       | hst038.08 | 1.0000           | 0.0026      | 0.9947           |
| 97        | hmt008detail  | 1.0009           | 0.0052      | 1.0085           | 154       | hst038.09 | 1.0000           | 0.0033      | 0.9939           |
| 98        | hmt010.15mil  | 1.0026           | 0.0072      | 0.9949           | 155       | hst038.10 | 1.0000           | 0.0026      | 0.9934           |
| 99        | hmt010.7.5mil | 1.0030           | 0.0072      | 0.9825           | 156       | hst038.11 | 1.0000           | 0.0025      | 0.9929           |
| 100       | hmt013.15mil  | 0.9983           | 0.0020      | 0.9944           | 157       | hst038.12 | 1.0000           | 0.0025      | 0.9931           |
| 101       | hmt013.625in  | 1.0021           | 0.0022      | 1.0017           | 158       | hst038.13 | 1.0000           | 0.0050      | 0.9971           |
| 102       | hmt014simple  | 0.9939           | 0.0015      | 0.9973           | 159       | hst038.14 | 1.0000           | 0.0050      | 0.9975           |
| 103       | hst001.01     | 1.0004           | 0.0060      | 0.9958           | 160       | hst038.15 | 1.0000           | 0.0050      | 0.9976           |
| 104       | hst001.02     | 1.0021           | 0.0072      | 0.9925           | 161       | hst038.16 | 1.0000           | 0.0050      | 0.9976           |
| 105       | hst001.03     | 1.0003           | 0.0035      | 0.9982           | 162       | hst038.17 | 1.0000           | 0.0026      | 0.9937           |
| 106       | hst001.04     | 1.0008           | 0.0053      | 0.9946           | 163       | hst038.18 | 1.0000           | 0.0032      | 0.9935           |
| 107       | hst001.05     | 1.0001           | 0.0049      | 0.9963           | 164       | hst038.19 | 1.0000           | 0.0032      | 0.9935           |
| 108       | hst001.06     | 1.0002           | 0.0046      | 0.9997           | 165       | hst038.20 | 1.0000           | 0.0032      | 0.9949           |
| 109       | hst001.07     | 1.0008           | 0.0040      | 0.9957           | 166       | hst038.21 | 1.0000           | 0.0025      | 0.9933           |
| 110       | hst001.08     | 0.9998           | 0.0038      | 0.9946           | 167       | hst038.22 | 1.0000           | 0.0027      | 0.9937           |
| 111       | hst001.09     | 1.0008           | 0.0054      | 0.9908           | 168       | hst038.23 | 1.0000           | 0.0027      | 0.9945           |
| 112       | hst001.10     | 0.9993           | 0.0054      | 0.9899           | 169       | hst038.24 | 1.0000           | 0.0026      | 0.9934           |
| 113       | hst002.01     | 1.0025           | 0.0058      | 0.9994           | 170       | hst038.25 | 1.0000           | 0.0032      | 0.9938           |
| 114       | hst002.02     | 1.0028           | 0.0058      | 1.0044           | 171       | hst038.26 | 1.0000           | 0.0032      | 0.9943           |
| 115       | hst002.03     | 1.0033           | 0.0068      | 0.9958           | 172       | hst038.27 | 1.0000           | 0.0032      | 0.9943           |
| 116       | hst002.04     | 1.0034           | 0.0069      | 1.0007           | 173       | hst038.28 | 1.0000           | 0.0025      | 0.9939           |
| 117       | hst002.05     | 1.0018           | 0.0044      | 1.0025           | 174       | hst038.29 | 1.0000           | 0.0025      | 1.0406           |
| 118       | hst002.06     | 1.0023           | 0.0041      | 1.0058           | 175       | hst038.30 | 1.0000           | 0.0027      | 1.0033           |
| 119       | hst002.07     | 1.0025           | 0.0050      | 0.9974           | 176       | hst039c2  | 1.0000           | 0.0051      | 1.0251           |
| 120       | hst002.08     | 1.0030           | 0.0055      | 1.0032           | 177       | hst042.1  | 0.9957           | 0.0039      | 0.9960           |
| 121       | hst002.09     | 1.0012           | 0.0046      | 0.9985           | 178       | hst042.2  | 0.9965           | 0.0036      | 0.9956           |
| 122       | hst002.10     | 1.0024           | 0.0050      | 1.0036           | 179       | hst042.3  | 0.9994           | 0.0028      | 1.0012           |
| 123       | hst002.11     | 1.0017           | 0.0038      | 1.0002           | 180       | hst042.4  | 1.0000           | 0.0034      | 1.0017           |
| 124       | hst002.12     | 1.0027           | 0.0050      | 1.0053           | 181       | hst042.5  | 1.0000           | 0.0034      | 1.0008           |
| 125       | hst002.13     | 1.0025           | 0.0055      | 0.9981           | 182       | hst042.6  | 1.0000           | 0.0037      | 0.9997           |
| 126       | hst002.14     | 1.0031           | 0.0066      | 0.9981           | 183       | hst042.7  | 1.0000           | 0.0036      | 0.9998           |
| 127       | hst004.1      | 1.0000           | 0.0033      | 0.9870           | 184       | hst042.8  | 1.0000           | 0.0035      | 1.0011           |

Case 5 of the hmt003 series benchmarks calculates high. For this case, the evaluators report about 0.9% difference between calculated and measured values as well.

The benchmark case hst038 case 29 exhibits a large difference between the measured and calculated  $k_{\text{eff}}$  values. Evaluators of this series also obtain very large discrepancies and indicate that the cause of this large difference for case 29 is unknown.

The benchmark case hst039 case 2 also exhibits a large difference between the measured and calculated  $k_{\text{eff}}$  values. Sample calculation results provided by the evaluators show similar large deviations for hst039 series benchmarks.

### 3.2. IEU

This group consists of 18 IEU systems. The calculated  $k_{\text{eff}}$  values and percent differences are shown in Fig. 2 to identify cases that show poor agreement. Table 2 lists the benchmark filenames,  $k_{\text{eff}}$  values, and KENO calculated  $k_{\text{eff}}$  values.

The agreement for all benchmark problems in this group is very good with an average percent difference of 0.04.

### 3.3. LEU

This group consists of 225 LEU systems. The calculated  $k_{\text{eff}}$  values and percent differences are shown in Fig. 3 to identify cases that show poor agreement. Table 3 lists the benchmark filenames,  $k_{\text{eff}}$  values, and KENO calculated  $k_{\text{eff}}$  values.

The agreement for all benchmark problems in this group is good; the average percent difference of -0.13. It is worth noting that the lct003 series benchmarks are underestimated. For this series of benchmarks, the evaluators also note that all cases are underpredicted by as much as 1% using various codes and data sets.

### 3.4. MOX

This group consists of 45 MOX systems. The calculated  $k_{\text{eff}}$  values and percent differences are shown in Fig. 4 to identify cases that show poor agreement. Table 4 lists the benchmark filenames,  $k_{\text{eff}}$  values, and KENO calculated  $k_{\text{eff}}$  values.

Cases 1 through 6 of the mct012 series benchmarks are poorly calculated. A review of the evaluations for these benchmarks revealed that evaluators also observed large differences between expected and calculated  $k_{\text{eff}}$  values for this set (cases 1 through 6 are in set I of mct012 series of benchmarks). The reason for large deviations for this set of benchmarks is not known. However, evaluators believe it may be due to the plutonium isotopes. Cases 31 through 33 also exhibit large differences. This behavior is not observed by the evaluators. Although the differences are large, the  $k_{\text{eff}}$  values are within  $3\sigma$  of each other. Large differences in cases 31 through 33 are attributed to the large benchmark uncertainties.

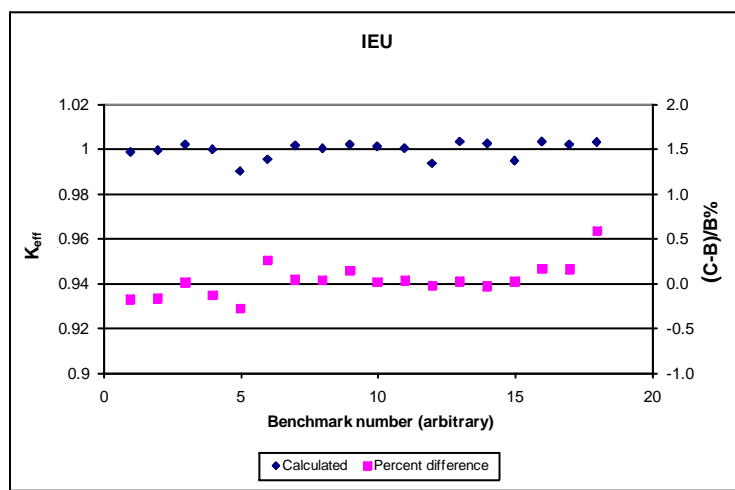


Fig. 2. Calculated  $k_{\text{eff}}$  values and percent differences for IEU benchmarks.

Table 2  
Calculated  $k_{\text{eff}}$  values and percent differences for IEU benchmarks

| Benchmark |           |                  |             | KENO-CE          | Benchmark |                |                  |             | KENO-CE          |
|-----------|-----------|------------------|-------------|------------------|-----------|----------------|------------------|-------------|------------------|
| No.       | Name      | $k_{\text{eff}}$ | Uncertainty | $k_{\text{eff}}$ | No.       | Name           | $k_{\text{eff}}$ | Uncertainty | $k_{\text{eff}}$ |
| 1         | ict002.1  | 1.0014           | 0.0039      | 0.9986           | 11        | imf002.1       | 1.0000           | 0.0030      | 1.0003           |
| 2         | ict002.2  | 1.0019           | 0.0040      | 0.9993           | 12        | imf007.twozone | 0.9948           | 0.0013      | 0.9936           |
| 3         | ict002.3  | 1.0017           | 0.0044      | 1.0018           | 13        | imf-007 detail | 1.0045           | 0.0007      | 1.0033           |
| 4         | ict002.4  | 1.0019           | 0.0044      | 0.9997           | 14        | imf-007 simple | 1.0045           | 0.0007      | 1.0025           |
| 5         | ict002.5  | 1.0014           | 0.0043      | 0.9900           | 15        | imf010.1       | 0.9954           | 0.0024      | 0.9946           |
| 6         | ict002.6  | 1.0016           | 0.0044      | 0.9954           | 16        | imf012.1       | 1.0007           | 0.0027      | 1.0033           |
| 7         | imf001.1i | 0.9989           | 0.0009      | 1.0014           | 17        | imf014.1       | 0.9958           | 0.0022      | 1.0019           |
| 8         | imf001.2i | 0.9997           | 0.0009      | 1.0001           | 18        | imf014.2       | 0.9927           | 0.0022      | 1.0030           |
| 9         | imf001.3i | 0.9993           | 0.0003      | 1.0019           |           |                |                  |             |                  |
| 10        | imf001.4i | 1.0002           | 0.0003      | 1.0010           |           |                |                  |             |                  |

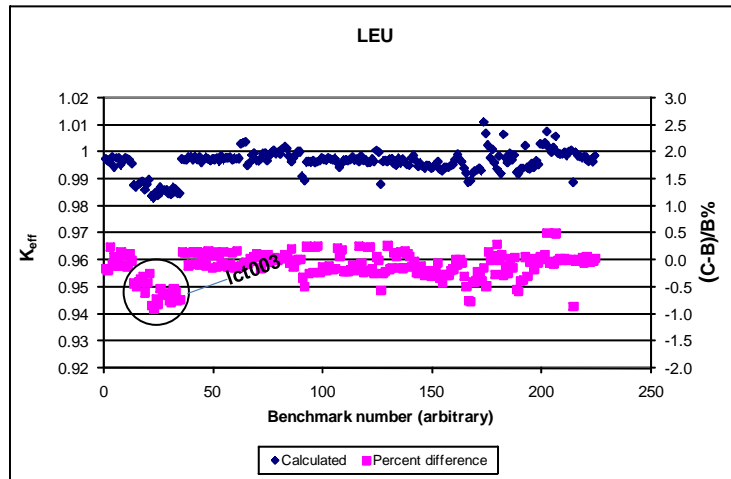


Fig. 3. Calculated  $k_{\text{eff}}$  values and percent differences for LEU benchmarks.

Table 3  
Calculated  $k_{\text{eff}}$  values and percent differences for LEU benchmarks

| Benchmark |           |                  |             | KENO-CE          | Benchmark |           |                  |             | KENO-CE          |
|-----------|-----------|------------------|-------------|------------------|-----------|-----------|------------------|-------------|------------------|
| No.       | Name      | $k_{\text{eff}}$ | Uncertainty | $k_{\text{eff}}$ | No.       | Name      | $k_{\text{eff}}$ | Uncertainty | $k_{\text{eff}}$ |
| 1         | lct001.1  | 1.0000           | 0.0031      | 0.9974           | 16        | lct003.03 | 1.0000           | 0.0039      | 0.9880           |
| 2         | lct001.2  | 0.9998           | 0.0030      | 0.9968           | 17        | lct003.04 | 1.0000           | 0.0039      | 0.9886           |
| 3         | lct001.3  | 0.9998           | 0.0030      | 0.9961           | 18        | lct003.05 | 1.0000           | 0.0039      | 0.9890           |
| 4         | lct001.4  | 0.9998           | 0.0030      | 0.9980           | 19        | lct003.06 | 1.0000           | 0.0039      | 0.9860           |
| 5         | lct001.5  | 0.9998           | 0.0030      | 0.9944           | 20        | lct003.07 | 1.0000           | 0.0039      | 0.9879           |
| 6         | lct001.6  | 0.9998           | 0.0030      | 0.9977           | 21        | lct003.08 | 1.0000           | 0.0039      | 0.9896           |
| 7         | lct001.7  | 0.9998           | 0.0031      | 0.9977           | 22        | lct003.09 | 1.0000           | 0.0039      | 0.9837           |
| 8         | lct001.8  | 0.9998           | 0.0030      | 0.9952           | 23        | lct003.10 | 1.0000           | 0.0039      | 0.9830           |
| 9         | lct002.1  | 0.9997           | 0.0020      | 0.9964           | 24        | lct003.11 | 1.0000           | 0.0039      | 0.9849           |
| 10        | lct002.2  | 0.9997           | 0.0020      | 0.9978           | 25        | lct003.12 | 1.0000           | 0.0039      | 0.9838           |
| 11        | lct002.3  | 0.9997           | 0.0020      | 0.9974           | 26        | lct003.13 | 1.0000           | 0.0039      | 0.9868           |
| 12        | lct002.4  | 0.9997           | 0.0018      | 0.9971           | 27        | lct003.14 | 1.0000           | 0.0039      | 0.9856           |
| 13        | lct002.5  | 0.9997           | 0.0019      | 0.9956           | 28        | lct003.15 | 1.0000           | 0.0039      | 0.9859           |
| 14        | lct003.01 | 1.0000           | 0.0039      | 0.9877           | 29        | lct003.16 | 1.0000           | 0.0039      | 0.9858           |
| 15        | lct003.02 | 1.0000           | 0.0039      | 0.9871           | 30        | lct003.17 | 1.0000           | 0.0039      | 0.9846           |

Table 3  
Calculated  $k_{\text{eff}}$  values and percent differences for LEU benchmarks (continued)

| Benchmark |           |                  |             | KENO-CE          | Benchmark |           |                  |             | KENO-CE          |
|-----------|-----------|------------------|-------------|------------------|-----------|-----------|------------------|-------------|------------------|
| No.       | Name      | $k_{\text{eff}}$ | Uncertainty | $k_{\text{eff}}$ | No.       | Name      | $k_{\text{eff}}$ | Uncertainty | $k_{\text{eff}}$ |
| 31        | lct003.18 | 1.0000           | 0.0039      | 0.9842           | 82        | lct010-20 | 1.0000           | 0.0028      | 1.0012           |
| 32        | lct003.19 | 1.0000           | 0.0039      | 0.9868           | 83        | lct010-21 | 1.0000           | 0.0028      | 1.0018           |
| 33        | lct003.20 | 1.0000           | 0.0039      | 0.9863           | 84        | lct010-22 | 1.0000           | 0.0028      | 1.0013           |
| 34        | lct003.21 | 1.0000           | 0.0039      | 0.9846           | 85        | lct010-23 | 1.0000           | 0.0028      | 0.9984           |
| 35        | lct003.22 | 1.0000           | 0.0039      | 0.9847           | 86        | lct010-24 | 1.0000           | 0.0028      | 0.9964           |
| 36        | lct009-01 | 1.0000           | 0.0021      | 0.9973           | 87        | lct010-25 | 1.0000           | 0.0028      | 0.9977           |
| 37        | lct009-02 | 1.0000           | 0.0021      | 0.9970           | 88        | lct010-26 | 1.0000           | 0.0028      | 0.9989           |
| 38        | lct009-03 | 1.0000           | 0.0021      | 0.9971           | 89        | lct010-27 | 1.0000           | 0.0028      | 1.0001           |
| 39        | lct009-04 | 1.0000           | 0.0021      | 0.9980           | 90        | lct010-28 | 1.0000           | 0.0028      | 1.0000           |
| 40        | lct009-05 | 1.0000           | 0.0021      | 0.9982           | 91        | lct010-29 | 1.0000           | 0.0028      | 0.9910           |
| 41        | lct009-06 | 1.0000           | 0.0021      | 0.9972           | 92        | lct010-30 | 1.0000           | 0.0028      | 0.9893           |
| 42        | lct009-07 | 1.0000           | 0.0021      | 0.9982           | 93        | lct016.01 | 1.0000           | 0.0031      | 0.9962           |
| 43        | lct009-08 | 1.0000           | 0.0021      | 0.9972           | 94        | lct016.02 | 1.0000           | 0.0031      | 0.9964           |
| 44        | lct009-09 | 1.0000           | 0.0021      | 0.9981           | 95        | lct016.03 | 1.0000           | 0.0031      | 0.9962           |
| 45        | lct009-10 | 1.0000           | 0.0021      | 0.9962           | 96        | lct016.04 | 1.0000           | 0.0031      | 0.9966           |
| 46        | lct009-11 | 1.0000           | 0.0021      | 0.9970           | 97        | lct016.05 | 1.0000           | 0.0031      | 0.9961           |
| 47        | lct009-12 | 1.0000           | 0.0021      | 0.9979           | 98        | lct016.06 | 1.0000           | 0.0031      | 0.9963           |
| 48        | lct009-13 | 1.0000           | 0.0021      | 0.9974           | 99        | lct016.07 | 1.0000           | 0.0031      | 0.9967           |
| 49        | lct009-14 | 1.0000           | 0.0021      | 0.9966           | 100       | lct016.08 | 1.0000           | 0.0031      | 0.9976           |
| 50        | lct009-15 | 1.0000           | 0.0021      | 0.9975           | 101       | lct016.09 | 1.0000           | 0.0031      | 0.9972           |
| 51        | lct009-16 | 1.0000           | 0.0021      | 0.9972           | 102       | lct016.10 | 1.0000           | 0.0031      | 0.9970           |
| 52        | lct009-17 | 1.0000           | 0.0021      | 0.9977           | 103       | lct016.11 | 1.0000           | 0.0031      | 0.9978           |
| 53        | lct009-18 | 1.0000           | 0.0021      | 0.9965           | 104       | lct016.12 | 1.0000           | 0.0031      | 0.9973           |
| 54        | lct009-19 | 1.0000           | 0.0021      | 0.9984           | 105       | lct016.13 | 1.0000           | 0.0031      | 0.9972           |
| 55        | lct009-20 | 1.0000           | 0.0021      | 0.9973           | 106       | lct016.14 | 1.0000           | 0.0031      | 0.9975           |
| 56        | lct009-21 | 1.0000           | 0.0021      | 0.9978           | 107       | lct016.15 | 1.0000           | 0.0031      | 0.9960           |
| 57        | lct009-22 | 1.0000           | 0.0021      | 0.9978           | 108       | lct016.16 | 1.0000           | 0.0031      | 0.9943           |
| 58        | lct009-23 | 1.0000           | 0.0021      | 0.9981           | 109       | lct016.17 | 1.0000           | 0.0031      | 0.9956           |
| 59        | lct009-24 | 1.0000           | 0.0021      | 0.9970           | 110       | lct016.18 | 1.0000           | 0.0031      | 0.9969           |
| 60        | lct009-25 | 1.0000           | 0.0021      | 0.9975           | 111       | lct016.19 | 1.0000           | 0.0031      | 0.9969           |
| 61        | lct009-26 | 1.0000           | 0.0021      | 0.9974           | 112       | lct016.20 | 1.0000           | 0.0031      | 0.9968           |
| 62        | lct009-27 | 1.0000           | 0.0021      | 0.9976           | 113       | lct016.21 | 1.0000           | 0.0031      | 0.9972           |
| 63        | lct010-01 | 1.0000           | 0.0021      | 1.0029           | 114       | lct016.22 | 1.0000           | 0.0031      | 0.9980           |
| 64        | lct010-02 | 1.0000           | 0.0021      | 1.0034           | 115       | lct016.23 | 1.0000           | 0.0031      | 0.9970           |
| 65        | lct010-03 | 1.0000           | 0.0021      | 1.0037           | 116       | lct016.24 | 1.0000           | 0.0031      | 0.9973           |
| 66        | lct010-04 | 1.0000           | 0.0021      | 0.9950           | 117       | lct016.25 | 1.0000           | 0.0031      | 0.9963           |
| 67        | lct010-05 | 1.0000           | 0.0021      | 0.9961           | 118       | lct016.26 | 1.0000           | 0.0031      | 0.9984           |
| 68        | lct010-06 | 1.0000           | 0.0021      | 0.9988           | 119       | lct016.27 | 1.0000           | 0.0031      | 0.9967           |
| 69        | lct010-07 | 1.0000           | 0.0021      | 0.9995           | 120       | lct016.28 | 1.0000           | 0.0031      | 0.9969           |
| 70        | lct010-08 | 1.0000           | 0.0021      | 0.9969           | 121       | lct016.29 | 1.0000           | 0.0031      | 0.9962           |
| 71        | lct010-09 | 1.0000           | 0.0021      | 0.9966           | 122       | lct016.30 | 1.0000           | 0.0031      | 0.9961           |
| 72        | lct010-10 | 1.0000           | 0.0021      | 0.9974           | 123       | lct016.31 | 1.0000           | 0.0031      | 0.9973           |
| 73        | lct010-11 | 1.0000           | 0.0021      | 0.9994           | 124       | lct016.32 | 1.0000           | 0.0031      | 0.9965           |
| 74        | lct010-12 | 1.0000           | 0.0021      | 0.9995           | 125       | lct017-01 | 1.0000           | 0.0031      | 1.0005           |
| 75        | lct010-13 | 1.0000           | 0.0021      | 0.9967           | 126       | lct017-02 | 1.0000           | 0.0031      | 0.9999           |
| 76        | lct010-14 | 1.0000           | 0.0028      | 0.9985           | 127       | lct017-03 | 1.0000           | 0.0031      | 0.9880           |
| 77        | lct010-15 | 1.0000           | 0.0028      | 0.9999           | 128       | lct017-10 | 1.0000           | 0.0031      | 0.9965           |
| 78        | lct010-16 | 1.0000           | 0.0028      | 1.0004           | 129       | lct017-11 | 1.0000           | 0.0031      | 0.9968           |
| 79        | lct010-17 | 1.0000           | 0.0028      | 0.9993           | 130       | lct017-12 | 1.0000           | 0.0031      | 0.9964           |
| 80        | lct010-18 | 1.0000           | 0.0028      | 0.9999           | 131       | lct017-13 | 1.0000           | 0.0031      | 0.9972           |
| 81        | lct010-19 | 1.0000           | 0.0028      | 0.9992           | 132       | lct017-14 | 1.0000           | 0.0031      | 0.9975           |

Table 3  
Calculated  $k_{\text{eff}}$  values and percent differences for LEU benchmarks (continued)

| Benchmark |           |                  |             | KENO-CE          | Benchmark |            |                  |             | KENO-CE          |
|-----------|-----------|------------------|-------------|------------------|-----------|------------|------------------|-------------|------------------|
| No.       | Name      | $k_{\text{eff}}$ | Uncertainty | $k_{\text{eff}}$ | No.       | Name       | $k_{\text{eff}}$ | Uncertainty | $k_{\text{eff}}$ |
| 133       | lct017-15 | 1.0000           | 0.0028      | 0.9957           | 180       | lst03c2    | 0.9993           | 0.0042      | 0.9937           |
| 134       | lct017-16 | 1.0000           | 0.0028      | 0.9951           | 181       | lst03c3    | 0.9995           | 0.0042      | 0.9984           |
| 135       | lct017-17 | 1.0000           | 0.0028      | 0.9976           | 182       | lst03c4    | 0.9995           | 0.0042      | 0.9920           |
| 136       | lct017-18 | 1.0000           | 0.0028      | 0.9959           | 183       | lst03c5    | 0.9997           | 0.0048      | 1.0065           |
| 137       | lct017-19 | 1.0000           | 0.0028      | 0.9974           | 184       | lst03c6    | 0.9999           | 0.0049      | 0.9977           |
| 138       | lct017-20 | 1.0000           | 0.0028      | 0.9959           | 185       | lst03c7    | 0.9994           | 0.0049      | 0.9960           |
| 139       | lct017-21 | 1.0000           | 0.0028      | 0.9954           | 186       | lst03c8    | 0.9993           | 0.0052      | 0.9995           |
| 140       | lct017-22 | 1.0000           | 0.0028      | 0.9949           | 187       | lst03c9    | 0.9996           | 0.0052      | 0.9971           |
| 141       | lct017-23 | 1.0000           | 0.0028      | 0.9976           | 188       | lst04-R01  | 0.9994           | 0.0008      | 0.9988           |
| 142       | lct017-24 | 1.0000           | 0.0028      | 0.9987           | 189       | lst04-R29  | 0.9999           | 0.0009      | 0.9924           |
| 143       | lct017-25 | 1.0000           | 0.0028      | 0.9968           | 190       | lst04-R33  | 0.9999           | 0.0009      | 0.9920           |
| 144       | lct039.01 | 1.0000           | 0.0014      | 0.9946           | 191       | lst04-R34  | 0.9999           | 0.0010      | 0.9937           |
| 145       | lct039.02 | 1.0000           | 0.0014      | 0.9958           | 192       | lst04-R46  | 0.9999           | 0.0010      | 0.9939           |
| 146       | lct039.03 | 1.0000           | 0.0014      | 0.9946           | 193       | lst04-R51  | 0.9994           | 0.0011      | 1.0023           |
| 147       | lct039.04 | 1.0000           | 0.0014      | 0.9941           | 194       | lst04-R54  | 0.9996           | 0.0011      | 0.9941           |
| 148       | lct039.05 | 1.0000           | 0.0014      | 0.9950           | 195       | lst07-R14  | 0.9961           | 0.0009      | 0.9936           |
| 149       | lct039.06 | 1.0000           | 0.0014      | 0.9948           | 196       | lst07-R30  | 0.9973           | 0.0009      | 0.9957           |
| 150       | lct039.07 | 1.0000           | 0.0014      | 0.9939           | 197       | lst07-R32  | 0.9985           | 0.0010      | 0.9944           |
| 151       | lct039.08 | 1.0000           | 0.0014      | 0.9945           | 198       | lst07-R36  | 0.9988           | 0.0011      | 0.9966           |
| 152       | lct039.09 | 1.0000           | 0.0014      | 0.9949           | 199       | lst07-R49  | 0.9983           | 0.0011      | 0.9952           |
| 153       | lct039.10 | 1.0000           | 0.0014      | 0.9964           | 200       | lst16-R105 | 0.9996           | 0.0013      | 1.0029           |
| 154       | lct039.11 | 1.0000           | 0.0014      | 0.9936           | 201       | lst16-R113 | 0.9999           | 0.0013      | 1.0027           |
| 155       | lct039.12 | 1.0000           | 0.0014      | 0.9928           | 202       | lst16-R125 | 0.9994           | 0.0014      | 1.0033           |
| 156       | lct039.13 | 1.0000           | 0.0014      | 0.9943           | 203       | lst16-R129 | 0.9996           | 0.0014      | 1.0075           |
| 157       | lct039.14 | 1.0000           | 0.0014      | 0.9942           | 204       | lst16-R131 | 0.9995           | 0.0014      | 1.0016           |
| 158       | lct039.15 | 1.0000           | 0.0014      | 0.9942           | 205       | lst16-R140 | 0.9992           | 0.0015      | 0.9998           |
| 159       | lct039.16 | 1.0000           | 0.0014      | 0.9950           | 206       | lst16-R196 | 0.9994           | 0.0015      | 1.0016           |
| 160       | lct039.17 | 1.0000           | 0.0014      | 0.9953           | 207       | lst17-R104 | 0.9981           | 0.0013      | 1.0057           |
| 161       | lct051.01 | 1.0010           | 0.0020      | 0.9969           | 208       | lst17-R122 | 0.9986           | 0.0013      | 0.9995           |
| 162       | lct051.02 | 1.0010           | 0.0024      | 0.9990           | 209       | lst17-R123 | 0.9989           | 0.0014      | 0.9992           |
| 163       | lct051.09 | 1.0010           | 0.0019      | 0.9973           | 210       | lst17-R126 | 0.9992           | 0.0014      | 0.9992           |
| 164       | lct051.10 | 1.0010           | 0.0019      | 0.9964           | 211       | lst17-R130 | 0.9987           | 0.0015      | 0.9998           |
| 165       | lct051.11 | 1.0010           | 0.0019      | 0.9940           | 212       | lst17-R147 | 0.9996           | 0.0015      | 0.9986           |
| 166       | lct051.12 | 1.0010           | 0.0019      | 0.9921           | 213       | lst18c1    | 0.9992           | 0.0010      | 1.0001           |
| 167       | lct051.13 | 1.0010           | 0.0022      | 0.9889           | 214       | lst18c3    | 0.9996           | 0.0010      | 1.0006           |
| 168       | lct051.14 | 1.0010           | 0.0019      | 0.9892           | 215       | lst18c4    | 0.9997           | 0.0010      | 0.9888           |
| 169       | lct051.15 | 1.0010           | 0.0024      | 0.9920           | 216       | lst18c5    | 0.9992           | 0.0010      | 0.9999           |
| 170       | lct051.16 | 1.0010           | 0.0020      | 0.9928           | 217       | lst18c6    | 0.9996           | 0.0010      | 0.9986           |
| 171       | lct051.17 | 1.0010           | 0.0027      | 0.9932           | 218       | lst20-R216 | 0.9995           | 0.0010      | 0.9983           |
| 172       | lct051.18 | 1.0010           | 0.0021      | 0.9939           | 219       | lst20-R217 | 0.9996           | 0.0010      | 0.9980           |
| 173       | lct051.19 | 1.0010           | 0.0019      | 0.9931           | 220       | lst20-R220 | 0.9997           | 0.0012      | 0.9982           |
| 174       | lct019c1  | 1.0000           | 0.0063      | 1.0111           | 221       | lst20-R226 | 0.9998           | 0.0012      | 0.9980           |
| 175       | lct019c2  | 1.0000           | 0.0058      | 1.0067           | 222       | lst21-R215 | 0.9983           | 0.0009      | 0.9964           |
| 176       | lct019c3  | 1.0000           | 0.0061      | 1.0025           | 223       | lst21-R218 | 0.9985           | 0.0010      | 0.9970           |
| 177       | lmt001.1  | 0.9990           | 0.0057      | 0.9979           | 224       | lst21-R221 | 0.9989           | 0.0011      | 0.9963           |
| 178       | lst001    | 0.9991           | 0.0029      | 1.0008           | 225       | lst21-R223 | 0.9993           | 0.0012      | 0.9986           |
| 179       | lst03c1   | 0.9997           | 0.0039      | 0.9960           |           |            |                  |             |                  |

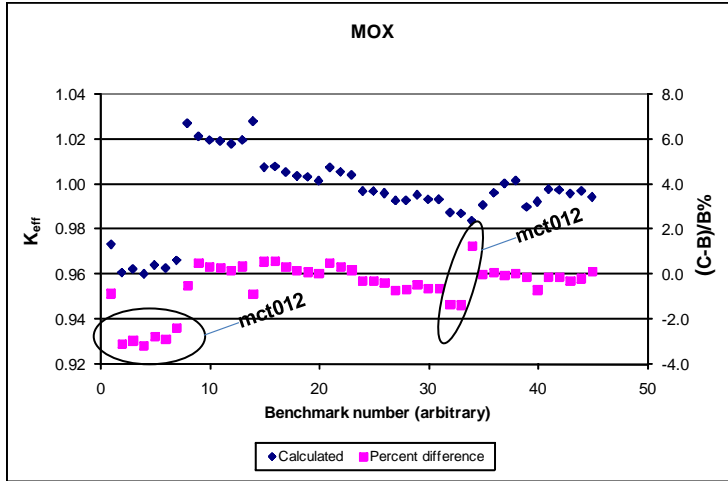


Fig. 4. Calculated  $k_{\text{eff}}$  values and percent differences for MOX benchmarks.

Table 4  
Calculated  $k_{\text{eff}}$  values and percent differences for MOX benchmarks

| Benchmark |           |                  |             | KENO-CE          | Benchmark |           |                  |             | KENO-CE          |
|-----------|-----------|------------------|-------------|------------------|-----------|-----------|------------------|-------------|------------------|
| No.       | Name      | $k_{\text{eff}}$ | Uncertainty | $k_{\text{eff}}$ | No.       | Name      | $k_{\text{eff}}$ | Uncertainty | $k_{\text{eff}}$ |
| 1         | mcf001    | 0.9866           | 0.0023      | 0.9733           | 24        | mct012.23 | 1.0007           | 0.0114      | 0.9968           |
| 2         | mct012.01 | 1.0052           | 0.0067      | 0.9608           | 25        | mct012.24 | 1.0007           | 0.0114      | 0.9968           |
| 3         | mct012.02 | 1.0052           | 0.0067      | 0.9623           | 26        | mct012.25 | 1.0007           | 0.0114      | 0.9959           |
| 4         | mct012.03 | 1.0052           | 0.0067      | 0.9600           | 27        | mct012.26 | 1.0007           | 0.0114      | 0.9926           |
| 5         | mct012.04 | 1.0052           | 0.0067      | 0.9641           | 28        | mct012.27 | 1.0007           | 0.0114      | 0.9928           |
| 6         | mct012.05 | 1.0052           | 0.0067      | 0.9627           | 29        | mct012.28 | 1.0007           | 0.0114      | 0.9951           |
| 7         | mct012.06 | 1.0052           | 0.0075      | 0.9662           | 30        | mct012.29 | 1.0007           | 0.0114      | 0.9933           |
| 8         | mct012.07 | 1.0053           | 0.0134      | 1.0270           | 31        | mct012.30 | 1.0007           | 0.0114      | 0.9933           |
| 9         | mct012.08 | 1.0053           | 0.0055      | 1.0213           | 32        | mct012.31 | 1.0017           | 0.0151      | 0.9873           |
| 10        | mct012.09 | 1.0053           | 0.0055      | 1.0196           | 33        | mct012.32 | 1.0017           | 0.0151      | 0.9870           |
| 11        | mct012.10 | 1.0053           | 0.0055      | 1.0192           | 34        | mct012.33 | 1.0017           | 0.0151      | 0.9837           |
| 12        | mct012.11 | 1.0053           | 0.0055      | 1.0179           | 35        | mmf011.1  | 0.9897           | 0.0023      | 0.9906           |
| 13        | mct012.12 | 1.0053           | 0.0055      | 1.0197           | 36        | mmf011.2  | 0.9998           | 0.0023      | 0.9960           |
| 14        | met012.13 | 1.0053           | 0.0158      | 1.0280           | 37        | mmf011.3  | 1.0018           | 0.0024      | 1.0002           |
| 15        | met012.14 | 1.0012           | 0.0086      | 1.0076           | 38        | mmf011.4  | 1.0012           | 0.0024      | 1.0016           |
| 16        | met012.15 | 1.0012           | 0.0086      | 1.0078           | 39        | mst007.1  | 1.0000           | 0.0043      | 0.9899           |
| 17        | met012.16 | 1.0012           | 0.0086      | 1.0053           | 40        | mst007.2  | 1.0000           | 0.0077      | 0.9922           |
| 18        | met012.17 | 1.0012           | 0.0086      | 1.0036           | 41        | mst007.3  | 1.0000           | 0.0046      | 0.9976           |
| 19        | met012.18 | 1.0012           | 0.0086      | 1.0031           | 42        | mst007.4  | 1.0000           | 0.0046      | 0.9975           |
| 20        | met012.19 | 1.0012           | 0.0086      | 1.0014           | 43        | mst007.5  | 1.0000           | 0.0091      | 0.9959           |
| 21        | met012.20 | 1.0014           | 0.0114      | 1.0073           | 44        | mst007.6  | 1.0000           | 0.0043      | 0.9969           |
| 22        | met012.21 | 1.0014           | 0.0120      | 1.0055           | 45        | mst007.7  | 1.0000           | 0.0034      | 0.9943           |
| 23        | met012.22 | 1.0014           | 0.0152      | 1.0040           |           |           |                  |             |                  |

### 3.5. Pu

This group consists of 30 Pu systems. The calculated  $k_{\text{eff}}$  values and percent differences are shown in Fig. 5 to identify cases that show poor agreement. Table 5 lists the benchmark filenames,  $k_{\text{eff}}$  values, and KENO calculated  $k_{\text{eff}}$  values.

Case pci001 is underpredicted by 1%, which is slightly less than the experimental uncertainty. However, the calculated and benchmark  $k_{\text{eff}}$  values are within  $3\sigma$  of each other.

Case pmi002.1 shows the largest discrepancy in this group. Similar large differences are also noted by the evaluators of this benchmark using various codes and data sets. It is speculated that the differences are due to the iron cross sections for this case (experiment name ZPR-6/10).

Case pst008.10 is overpredicted by more than 1%. Evaluators of the pst008 series benchmarks also report similar trends with various code and data sets.

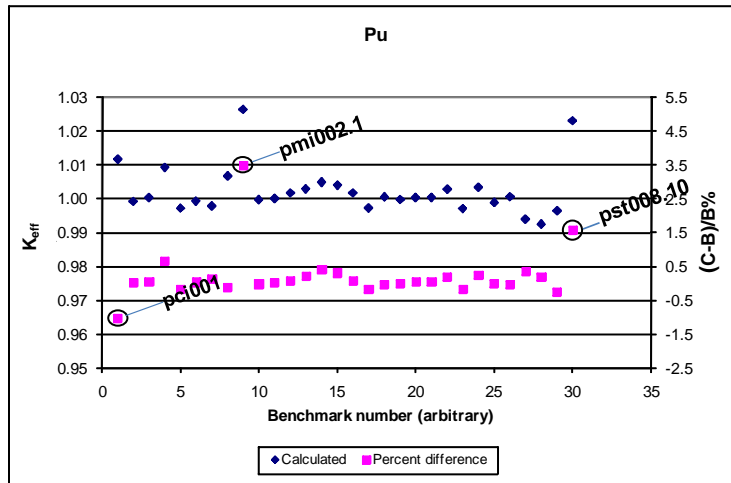


Fig. 5. Calculated  $k_{\text{eff}}$  values and percent differences for Pu benchmarks.

Table 5  
Calculated  $k_{\text{eff}}$  values and percent differences for Pu benchmarks

| No. | Name       | Benchmark        |             | KENO-CE | Benchmark        |             | KENO-CE |        |        |
|-----|------------|------------------|-------------|---------|------------------|-------------|---------|--------|--------|
|     |            | $k_{\text{eff}}$ | Uncertainty |         | $k_{\text{eff}}$ | Uncertainty |         |        |        |
| 1   | pci001     | 1.0000           | 0.0110      | 1.0116  | 16               | pst005.7    | 1.0000  | 0.0047 | 1.0018 |
| 2   | pmf001bare | 1.0000           | 0.0020      | 0.9992  | 17               | pst005.8    | 1.0000  | 0.0047 | 0.9972 |
| 3   | pmf002     | 1.0000           | 0.0020      | 1.0004  | 18               | pst005.9    | 1.0000  | 0.0047 | 1.0005 |
| 4   | pmf005     | 1.0000           | 0.0013      | 1.0093  | 19               | pst006.1    | 1.0000  | 0.0035 | 0.9998 |
| 5   | pmf006     | 1.0000           | 0.0030      | 0.9972  | 20               | pst006.2    | 1.0000  | 0.0035 | 1.0004 |
| 6   | pmf008.1   | 1.0000           | 0.0006      | 0.9993  | 21               | pst006.3    | 1.0000  | 0.0035 | 1.0005 |
| 7   | pmf012     | 1.0009           | 0.0021      | 0.9979  | 22               | pst007.02   | 1.0000  | 0.0047 | 1.0028 |
| 8   | pmf013     | 1.0034           | 0.0023      | 1.0068  | 23               | pst007.03   | 1.0000  | 0.0047 | 0.9971 |
| 9   | pmi002.1   | 0.9869           | 0.0026      | 1.0265  | 24               | pst007.05   | 1.0000  | 0.0047 | 1.0034 |
| 10  | pst005.1   | 1.0000           | 0.0047      | 0.9997  | 25               | pst007.06   | 1.0000  | 0.0047 | 0.9988 |
| 11  | pst005.2   | 1.0000           | 0.0047      | 1.0002  | 26               | pst007.07   | 1.0000  | 0.0047 | 1.0006 |
| 12  | pst005.3   | 1.0000           | 0.0047      | 1.0017  | 27               | pst007.08   | 1.0000  | 0.0047 | 0.9940 |
| 13  | pst005.4   | 1.0000           | 0.0047      | 1.0030  | 28               | pst007.09   | 1.0000  | 0.0047 | 0.9925 |
| 14  | pst005.5   | 1.0000           | 0.0047      | 1.0049  | 29               | pst007.10   | 1.0000  | 0.0047 | 0.9964 |
| 15  | pst005.6   | 1.0000           | 0.0047      | 1.0041  | 30               | pst008.10   | 1.0000  | 0.0037 | 1.0231 |

### 3.6. U-233

This group consists of 13 U-233 systems. The calculated  $k_{\text{eff}}$  values and percent differences are shown in Fig. 6 to identify cases that show poor agreement. Table 6 lists the benchmark filenames,  $k_{\text{eff}}$  values, and KENO calculated  $k_{\text{eff}}$  values.

For this group of benchmarks, the agreement between the benchmark and calculated values is excellent.

#### 4. Summary

More than 500 benchmark problems have been modeled and analyzed in this validation study. The benchmark problems have been divided into six groups: HEU, IEU, LEU, MOX, Pu, and U-233. The average percent difference between the calculated and benchmark  $k_{\text{eff}}$  values for the HEU group is 0.0. Although there are some benchmark cases in this group that are calculated poorly, calculations reported by the evaluators of these benchmarks using other code and data sets show similar poor agreement. Therefore, the performance of KENO and the associated ENDF/B-VII Release 0 continuous energy cross sections for HEU systems is deemed very good.

The average percent difference between the calculated and benchmark  $k_{\text{eff}}$  values for the IEU group is 0.04. The performance of KENO and the associated ENDF/B-VII Release 0 continuous energy cross sections for IEU systems is deemed very good.

The average percent difference between the calculated and benchmark  $k_{\text{eff}}$  values for the LEU group is -0.13. The performance of KENO and the associated ENDF/B-VII Release 0 continuous energy cross sections for LEU systems is deemed very good.

The average percent difference between the calculated and benchmark  $k_{\text{eff}}$  values for the MOX group is -0.5. The reason for this large average value is set I of the mct012 series benchmarks. Calculations using other code and data sets reported by the evaluators of these benchmarks show similar poor agreement. Therefore, the performance of KENO and the associated ENDF/B-VII Release 0 continuous energy cross sections for MOX systems is deemed very good.

The average percent difference between the calculated and benchmark  $k_{\text{eff}}$  values for the Pu group is 0.2. Although there are some benchmark cases in this group that calculate poorly, calculations using other code and data sets reported by the evaluators of these benchmarks show similar poor agreement. Therefore, the performance of KENO and the associated ENDF/B-VII Release 0 continuous energy cross sections for Pu systems is deemed very good.

Finally, the average percent difference between the calculated and benchmark  $k_{\text{eff}}$  values for the U-233 group is 0.0. The performance of KENO and the associated ENDF/B-VII Release 0 continuous energy cross sections for U-233 systems is deemed excellent.

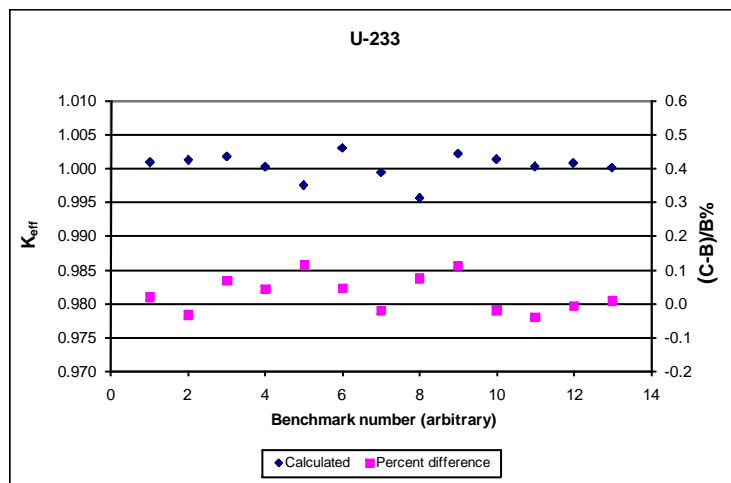


Fig. 6. Calculated  $k_{\text{eff}}$  values and percent differences for U-233 benchmarks.

Table 6  
Calculated  $k_{\text{eff}}$  values and percent differences for U-233 benchmarks

| Benchmark |          |                  |             | KENO-CE          | Benchmark |          |                  |             | KENO-CE          |
|-----------|----------|------------------|-------------|------------------|-----------|----------|------------------|-------------|------------------|
| No.       | Name     | $k_{\text{eff}}$ | Uncertainty | $k_{\text{eff}}$ | No.       | Name     | $k_{\text{eff}}$ | Uncertainty | $k_{\text{eff}}$ |
| 1         | uct001.1 | 1.0006           | 0.0027      | 1.0008           | 8         | uct001.8 | 1.0004           | 0.0028      | 0.9955           |
| 2         | uct001.2 | 1.0015           | 0.0025      | 1.0012           | 9         | ust001.1 | 1.0000           | 0.0031      | 1.0021           |
| 3         | uct001.3 | 1.0000           | 0.0024      | 1.0016           | 10        | ust001.2 | 1.0005           | 0.0033      | 1.0013           |
| 4         | uct001.4 | 1.0007           | 0.0025      | 1.0001           | 11        | ust001.3 | 1.0006           | 0.0033      | 1.0002           |
| 5         | uct001.5 | 1.0015           | 0.0026      | 0.9974           | 12        | ust001.4 | 0.9998           | 0.0033      | 1.0007           |
| 6         | uct001.6 | 1.0015           | 0.0028      | 1.0029           | 13        | ust001.5 | 0.9999           | 0.0033      | 1.0000           |
| 7         | uct001.7 | 0.9995           | 0.0027      | 0.9993           |           |          |                  |             |                  |

## References

- SCALE: A Modular Code System for Performing Standardized Computer Analysis for Licensing Evaluations, ORNL/TM-2005/39, Version 5.1, Vols. I-III, November 2006. Available from Radiation Safety Information Computational Center at Oak Ridge National Laboratory as CCC-732.
- Dunn, M.E., Greene, N.M. 2002. AMPX-2000: A Cross-Section Processing System for Generating Nuclear Data for Criticality Safety Applications. Trans. Am. Nucl. Soc. 86, 118–119.
- Goluoglu, S., Dunn, M.E., Greene, N.M., Petrie, L.M., and Hollenbach, D.F. 2007. Generation and Testing of the ENDF/B-VI Continuous-Energy Cross-Section Library for Use with Continuous-Energy Versions of KENO, Proc. of ICNC 2007, St. Petersburg, Russia.
- International Handbook of Evaluated Criticality Safety Benchmark Experiments, NEA/NSC/DOC(95)03, OECD-NEA, September, 2007.